Studies of Miscibility Behavior and Hydrogen Bonding in Blends of Poly(vinylphenol) and Poly(vinylpyrrolidone)

Shiao Wei Kuo and Feng Chih Chang*

Institute of Applied Chemistry, National Chiao Tung University, Hsin Chu, Taiwan

Received March 26, 2001; Revised Manuscript Received May 14, 2001

ABSTRACT: Polymer blends of poly(vinylphenol) (PVPh) with poly(vinylpyrrolidone) (PVP) were prepared by solution casting from the *N*,*N*-dimethylformamide (DMF) solution. Differential scanning calorimetry (DSC), Fourier transform infrared spectroscopy (FTIR), and solid-state nuclear magnetic resonance (NMR) were used to investigate the hydrogen bonding and miscibility behavior of the blend. This PVPh/PVP blend system has a single glass transition temperature over the entire composition range, indicating that this blend is able to form a miscible phase due to the formation of inter-hydrogen bonding between the hydroxyl of PVPh and the carbonyl of PVP. Furthermore, FTIR and solid-state NMR were used to study the hydrogen-bonding interaction between the PVPh hydroxyl group and the PVP carbonyl group at various compositions. According to the Painter−Coleman association model (PCAM), the interassociation constant for the PVPh/PVP blend is significantly higher than the self-association constant of PVPh, revealing that the tendency toward hydrogen bonding of the PVPh and PVP dominates the intra-hydrogen bonding of the PVPh in the mixture.

Introduction

It is well-known that most polymer blends are immiscible due to a high degree of polymerization, which predicts the small combinatorial entropy, based directly from a simple Flory−Huggins description of the thermodynamics theory. Therefore, to obtain a one-phase system in polymer blends, it is usually necessary to ensure that favorable specific intermolecular interaction exists between two base components of the blend, for example, hydrogen bonding.[1−3] This type of interaction has been widely described in terms of association model by Coleman et al.[4] This model is modified by the Flory−Huggins theory to include a free energy change associated with hydrogen bonding that has both entropic and enthalpic contribution. Furthermore, the interassociation equilibrium constant and its related enthalpy necessary to quantify this free energy can be calculated at various temperatures by FTIR according to the Painter−Coleman association model (PCAM).[4]

The strong interaction and miscible polymer blends provide attractive interest in polymer science due to strong economic incentives arising from their potential application. It has been demonstrated that poly(vinylpyrrolidone) is able to interact strongly with polymers of a wide variety of structure, such as poly(vinyl chloride),[5] poly(vinyl alcohol),[6] phenoxy,[7] and poly(vinylidene fluoride).[8] Generally, the specific interaction of polymer blends can be characterized by various techniques, including Fourier transform infrared spectroscopy[9−12] and solid-state NMR.[13−16]

The purpose of the present work is the study of the miscibility behavior and hydrogen bonding of PVPh/PVP blends. The analysis of the effect of hydrogen bonding on the miscibility will be investigated using differential scanning calorimetry (DSC), Fourier transform infrared spectroscopy, and solid-state NMR.

* To whom corresponding should be addressed. E-mail changfc@cc.nctu.edu.tw; Tel 886-3-5712121, ext. 56502; FAX 886-3-5723764.

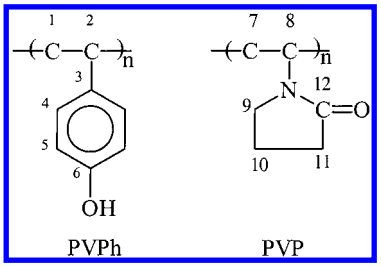

Figure 1. Chemical structures of PVPh and PVP and their atom numbering schemes.

Experimental Section

Materials. The poly(vinylphenol) (PVPh) with a M_w = 9000−10 000 were purchased from Polyscience Inc.. The poly(vinylpyrrolidone) (PVP) used in this study is from Aldrich with a M_w = 10 000. The chemical structures of PVPh and PVP are illustrated as follows in Figure 1.

Blend Preparation. Blends of PVPh/PVP with different compositions were prepared by solution blending. *N*,*N*-Dimethylformamide solution containing 5 wt % polymer mixture was stirred for 6−8 h, and the solution was allowed to evaporate slowly at 50 °C for 1 day. The film of the blend was then dried at 80 °C for 2 days to ensure total elimination of solvent.

Characterizations. *Differential Scanning Calorimetry*. The glass transition temperatures of the blend was performed using a DSC from Du-Pont (DSC-9000) with scan rate of 20 °C/min and temperature range 30−150 °C. The measurement was made using 5−10 mg sample on a DSC sample cell after the sample was quickly cooled to 30 °C from the melt of the first scan. The glass transition temperature was obtained as the inflection point of the jump heat capacity with scan rate of 20 °C/min and temperature range 30−250 °C.

*Infrared Spectroscopy***.** Infrared spectra were recorded on a Nicolet Avatar 320 FT-IR spectrophotometer, and 32 scans were collected with a spectral resolution 1 cm^{-1}. Infrared spectra of polymer blend films were determined by using the conventional NaCl disk method. The DMF solution containing the blend was cast onto NaCl disk and dried under conditions similar to that used in the bulk preparation. The film used in this study was sufficiently thin to obey the Beer−Lambert law. IR spectra recorded at elevated temperatures were obtained by using a cell mounted inside the temperature-controlled compartment of the spectrometer.

10.1021/ma010517a CCC: $20.00
Published on Web 06/19/2001

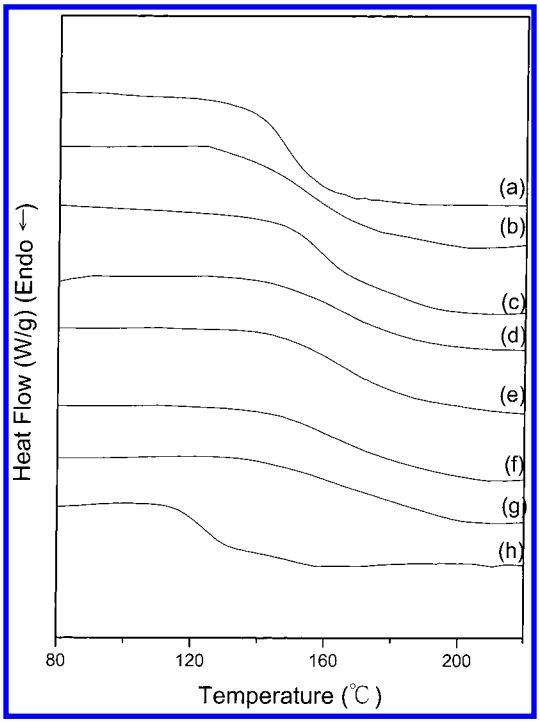

Figure 2. DSC scans of PVPh/PVP blends with different compositions: (a) 100/0, (b) 60/40, (c) 50/50, (d) 40/60, (e) 30/70, (f) 20/80, (g) 10/90, and (h) 0/100.

Solid-State NMR. High-resolution solid-state ^{13}C NMR experiments were carried out at room temperature using a Bruker DSX-400 spectrometer operating at resonance frequencies of 399.53 and 100.47 MHz for ^{1}H and ^{13}C, respectively. The ^{13}C CP/MAS spectra were measured with a 3.9 μs 90° pulse, with 3 s pulse delay time, acquisition time of 30 ms, and 2048 scans. All NMR spectra were taken at 300 K using broad-band proton decoupling and a normal cross-polarization pulse sequence. A magic angle sample spinning (MAS) rate of 5.4 kHz was used to avoid absorption overlapping. The proton spin−lattice relaxation time in the rotating frame ($T_{1\rho}^{H}$) was determined indirectly via carbon observation using a 90°−τ− spin lock pulse sequence prior to cross-polarization. The data acquisition was performed via ^{1}H decoupling and delay time (τ) ranging from 0.1 to 12 ms with a contact time of 1.0 ms.

Results and Discussion

Thermal Analyses. The DSC analysis is one of the convenient methods to determine the miscibility in polymer blends. Figure 2 shows the DSC thermograms of the PVPh/PVP blend with various compositions, revealing that all PVPh/PVP blend has only a single glass transition temperature. A single T_g strongly suggests that these are fully miscible blends with a homogeneous amphorous phase. Meanwhile, a single T_g higher than that of either individual polymer was observed. The large positive deviation indicates that the strong interaction exists between the two polymers. Over the years, a number of equations have been offered to predict the variation of the glass transition temperature of a miscible blend as a function of composition. The most popular equation is the Kwei equation[17] as follows:

$$T_g = \frac{W_1 T_{g1} + k W_2 T_{g2}}{W_1 + k W_2} + q W_1 W_2 \qquad (1)$$

where W_1 and W_2 are weight fractions of the compositions, T_{g1} and T_{g2} represent the corresponding glass transition temperatures, and k and q are fitting constants. Figure 3 shows the dependence of the T_g on the composition of the miscible PVPh/PVP blends, where the maximum deviation on the highest T_g is obtained when blend composition is at PVPh/PVP = 50/50. In addition, $k = 1$ and $q = 140$ are obtained from the nonlinear least-squares "best fit" values, where q is a parameter corresponding to the strength of hydrogen bonding in the blend, reflecting a balance between the breaking of the self-association and the forming of the interassociation hydrogen bonding. In this study, a positive q of 140 is obtained, indicating a strong intermolecular interaction between PVPh and PVP.

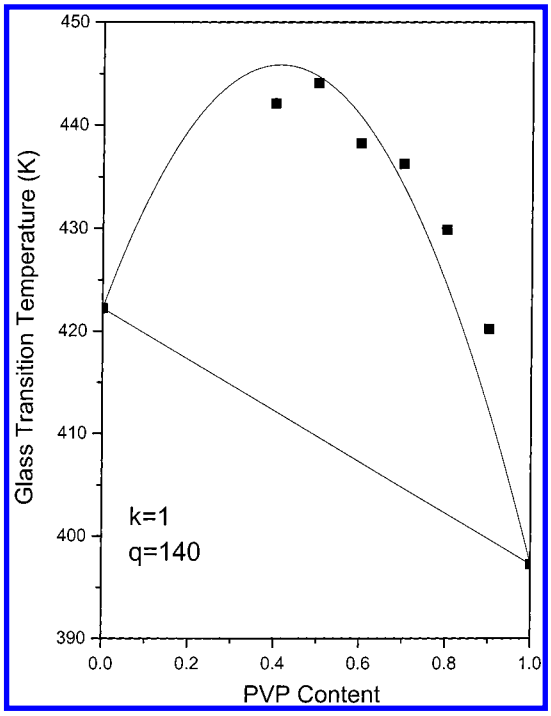

Figure 3. T_g vs composition curves based on (■) experimental data and (—) the Kwei equation.

Fourier Transform Infrared Spectroscopy Analyses. FTIR spectrometry has proven to be a very powerful technique to detect the intermolecular interaction between two polymers. The hydroxyl stretching range in the infrared spectrum is sensitive to the hydrogen-bonding formation. Figure 4 illustrates scale-expanded infrared spectra in the range 2700−4000 cm^{-1} of the PVPh/PVP blend measured at 150 °C. We choose 150 °C to measure experiment data because this temperature is above both components glass transition temperatures, and the DSC curves were experimentally obtained by quenching the samples from this temperature. Therefore, it is reasonable to characterize the specific interaction that the equilibrium condition is retained. The pure PVPh shows two distinct bands in the hydroxyl stretching region of the infrared spectra. Figure 4 shows a broad band centered at 3420 cm^{-1} and a shoulder at 3525 cm^{-1}, corresponding to the multimer hydrogen-bonded hydroxyl group and free hydroxyl group, respectively. The peak frequency of this broad band shifts to lower wavenumber with increasing PVP content. Meanwhile, the intensity of the free hydroxyl group decreases gradually with the increase of PVP content as would be expected. This result reflects a new distribution of hydrogen-bonding formation resulting from the competition between hydroxyl−hydroxyl and

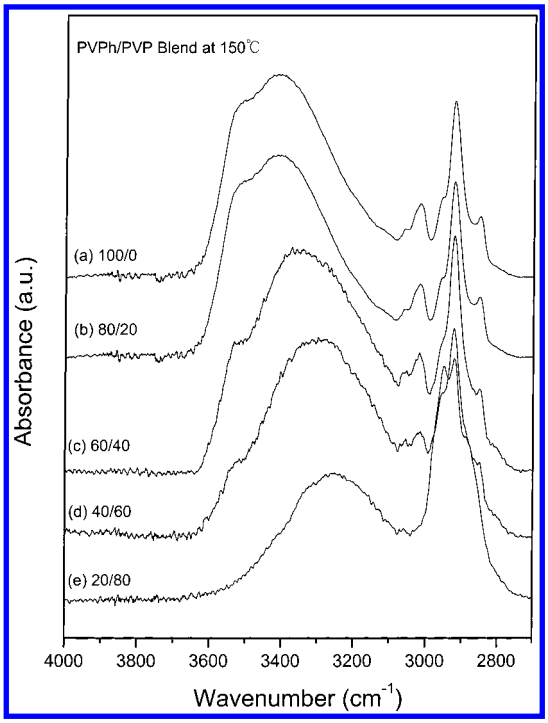

Figure 4. FTIR spectra recorded at 150 °C in the 2700−4000 cm^{-1} region for pure PVPh and various PVPh/PVP blends: (a) 100/0, (b) 80/20, (c) 60/40, (d) 40/60, and (e) 20/80.

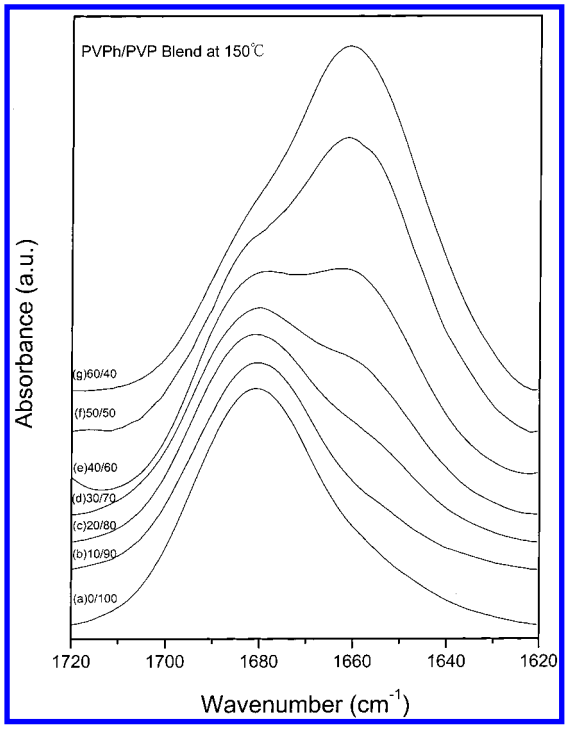

Figure 5. FTIR spectra recorded at 150 °C in the 1620−1720 cm^{-1} region for PVPh/PVP blends: (a) 0/100, (b) 10/90, (c) 20/80, (d) 30/70, (e) 40/60, (f) 50/50, and (g) 60/40.

hydroxyl−carbonyl interactions. It also reveals that the hydroxyl−carbonyl interaction predominates in PVP-rich blends, so that it is reasonable to assign the band at 3250 cm^{-1} as the hydroxyl group bonded to the carbonyl group. Coleman et al.[18] have used the frequency difference ($\Delta\nu$) between the hydrogen-bonded hydroxyl absorption and free hydroxyl absorption to investigate the average strength of the intermolecular interaction. Therefore, the hydroxyl−carbonyl interassociation ($\Delta\nu$ = 275 cm^{-1}) is stronger than the hydroxyl−hydroxyl self-association ($\Delta\nu$ = 105 cm^{-1}) interaction, and this result is consistent with the positive q value obtained in the Kwei equation.

Figure 5 presents FTIR spectra of the carbonyl stretching recorded at 150 °C ranging from 1620 to 1720 cm^{-1} for the blends with various compositions. The carbonyl stretching frequency splits into two bands at 1680 and 1660 cm^{-1}, corresponding to the free and the hydrogen-bonded carbonyl groups, which can be fitted well to the Gaussian function. The fraction of the hydrogen-bonded carbonyl group can be calculated by eq 2:[4]

$$f_b^{C=O} = \frac{A_b/1.3}{A_b/1.3 + A_f} \qquad (2)$$

A_f and A_b denote peak areas corresponding to the free and the hydrogen-bonded carbonyl groups, respectively. In this study, the ratio of the two absorptivities a_2/a_1 is equal to 1.3 according to previous infrared studies in hydroxyl−carbonyl interassociation.[19] Table 1 summarizes results from curve fitting, indicating that the hydrogen-bonded fraction of the carbonyl group increases with the increase of the PVPh content. The results obtained from the FTIR studies at 150 °C in the amphorous state are entirely consistent with a miscible blend system. In addition, the $W_{1/2}$ of the free carbonyl band from Table 1 increases with concentration of PVP,

Table 1. Curve Fitting of Fraction of Hydrogen-Bonding Results of the PVPh/PVP Blends at 150 °C

	free C=O			H-bonded C=O			
PVPh/PVP	ν, cm^{-1}	$W_{1/2}$, cm^{-1}	A_f (%)	ν, cm^{-1}	$W_{1/2}$, cm^{-1}	A_b (%)	fb (%)[a]
60/40	1686.2	16.8	17.32	1660.3	28.6	82.68	78.59
50/50	1684.3	18.4	29.32	1660.1	27.3	70.68	64.96
40/60	1685.3	19.2	40.69	1660.4	26.1	59.31	52.85
30/70	1683.5	23.0	55.08	1658.6	25.5	44.92	38.55
20/80	1683.1	23.5	68.50	1658.7	26.4	31.50	26.13
10/90	1683.1	25.1	85.30	1658.2	24.4	14.70	11.70

[a] fb = fraction of hydrogen bonding.

indicating that the pure PVP has strong transition dipole coupling between neighboring molecules or polymer segment, and the observed result is similar to the previous Hu et al. study.[19]

Solid-State NMR Analyses. Solid-state NMR spectroscopy provides further insight into the phase behavior and morphology of polymer blends involving the hydrogen bond formation. The ^{13}C CP/MAS spectra of PVPh, PVP, and their blends are shown in Figure 6. The pure PVPh has six resonance peaks, and the hydroxyl-substituted carbon in the phenolic ring (C-6) is at 153.2 ppm. Six peaks can be observed from the pure PVP, and the resonance peak at 176.5 ppm is from the carbonyl carbon (C-12). All other peak assignments assigned in Figure 6 are shown in Figure 1.

The spectra of these blends display significant changes in comparison with those of the pure polymer. Figure 7 shows that the chemical shift of the carbonyl carbon of the PVP increases with the increase of the PVPh content. The variation in the observed chemical shift (≒1.2 ppm) of the carbonyl carbon (C=O) indicates that the existence of a specific interaction between PVPh and PVP segments. It is well-known that the hydrogen bonding in polymer blends can affect the chemical environment of the neighboring molecules, causing a

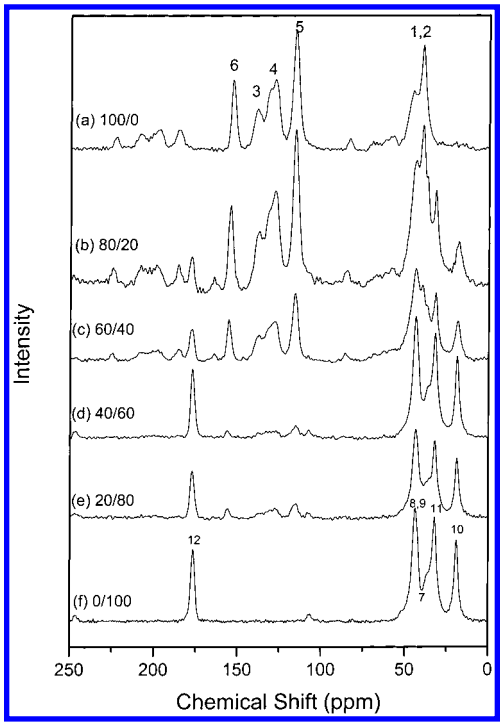

Figure 6. ^{13}C CPMAS spectra at room temperature for PVPh/PVP blends: (a) 100/0, (b) 80/20, (c) 60/40, (d) 40/60, (e) 20/80, and (f) 0/100.

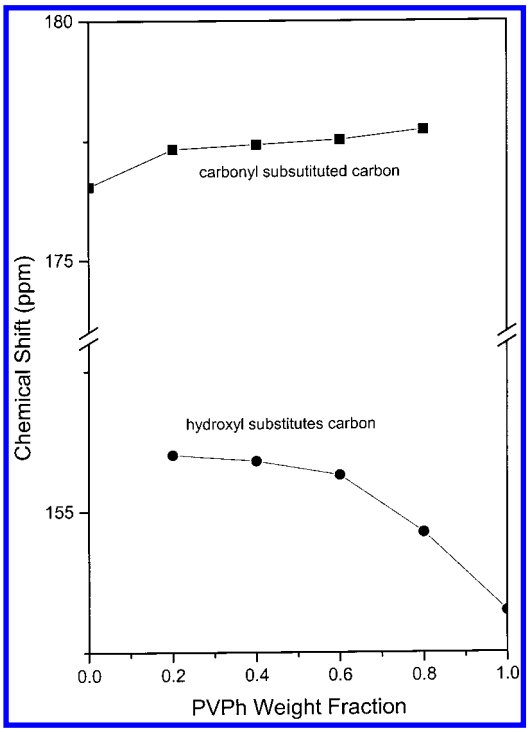

Figure 7. Composition dependence of the chemical shift of the carbonyl group (■) and the hydroxyl-substituted carbon (●) in the PVPh/PVP blends.

chemical shift to downfield. The hydroxyl-substituted carbon in phenolic ring (C-6) of pure PVPh is at 153.2 ppm; a downfield shift of 2.8 ppm is observed in the PVPh/PVP = 20/80 blend relative to the pure PVPh, implying strong intermolecular interassociation between the hydroxyl of PVPh and carbonyl of PVP. These results are also in good agreement with FTIR results and the T_g composition relationship based on the Kwei equation.

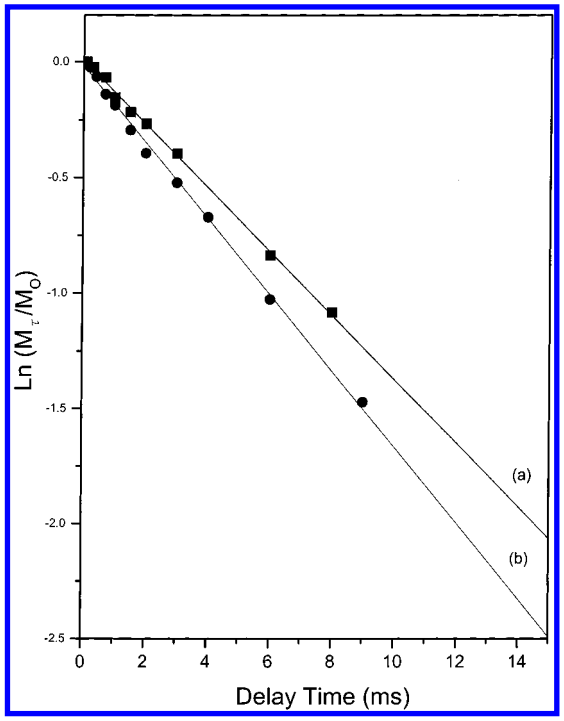

Figure 8. Semilogarithmic plots of the magnetization intensities of 115 ppm vs delay time for pure PVPh and PVPh/PVP blends at contact time of 1 ms: (a) pure PVPh; (b) 60/40.

The spin−lattice relaxation time in the rotating frame ($T_{1\rho}^{H}$) has widely been used to examine the homogeneity of PVPh/PVP blend on the molecular scale. The magnetization of resonance is expected to decay according to the following exponential function model by eq 3: according to the spin-locking mode employed in this study.

$$M_\tau = M_0 \exp(-\tau/T_{1\rho}^{H}) \tag{3}$$

where $T_{1\rho}^{H}$ is the spin−lattice relaxation time in the rotating frame, τ is the delay time used in the experiment, and M_τ is the corresponding resonance. $T_{1\rho}^{H}$ can be obtained from the slope of $\ln(M_\tau/M_0)$ vs τ. The $T_{1\rho}^{H}$ relaxation behaviors of these blends are shown in Figure 8 (PVPh, 115 ppm), revealing that both pure PVPh and the PVPh/PVP = 60/40 blend exhibit only single relaxation throughout all blends, indicating good miscibility and dynamic homogeneity in the PVPh phase. The maximum diffusive path length L can be estimated using the approximated eq 4[20−22]

$$L = (6DT)^{1/2} \tag{4}$$

For $T_{1\rho}^{H}$ of 5 ms and a effective spin diffusion coefficient, D, of 10^{-16} m^2 s^{-1}, the dimensions of these PVPh/PVP blends are below 2−3 nm in the amphorous phase.

Painter−Coleman Association Model Analyses. According to the Painter−Coleman association model, the quantity of the free energy contribution is due to the change in hydrogen bonding upon mixing. It is necessary to determine a set of equilibrium constants including self-association and interassociation and other properties of thermodynamics to predict the free energy and miscibility windows involving specific interactions. Table 2 summarizes these equilibrium constants and their related enthalpies, molar volumes, molecular weights, and solubility parameters of the PVPh/PVP

Table 2. Summary of the Self-Association and Interassociation Parameters of PVPh/PVP Blend

	K (25 °C)	ΔH (kcal/mol)
self-association[a]		
dimer formation K_2	21.0	−5.60
multimer formation K_B	66.8	−5.20
interassociation between PVPh and PVP[b]	6000.0	−6.04

polymer	molar vol (mL/mol)	mol wt (g/mol)	solubility parameter $(cal/mL)^{0.5}$	DP[d]
PVPh[c]	100.0	120.1	10.6	83
PVP[c]	73.6	115.1	11.0	86

[a] Reference 4. [b] Reference 19. [c] Estimated by using a group contribution method proposed by Coleman et al.[4] [d] Degree of polymerization.

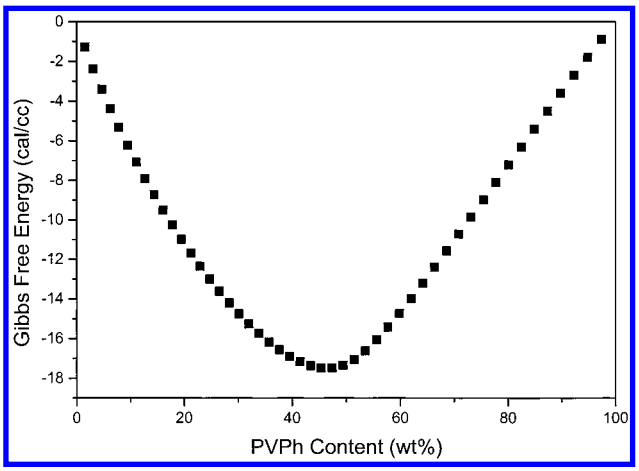

Figure 9. Calculated free energy of mixing against PVPh/PVP blend composition at 150 °C.

blend. K_2 and K_B represent the hydrogen-bonded dimer and multimer of the self-association of PVPh, respectively. The K_A reflects the extent of the hydrogen bonding between PVPh and PVP.

The observed $K_A = 6000$ is found to be much higher than $K_2 = 21.00$ from the hydroxyl dimer formation and $K_B = 66.80$ from the hydroxyl multimer formation. This result implies that the tendency toward forming the hydrogen bonding of the PVPh with PVP dominates over the self-association forming the intra-hydrogen bonding of the pure PVPh. Furthermore, this result is also in good agreement with T_g−compositional relationship based on the Kwei equation from both FTIR and NMR observations.

Prediction of Free Energy. Figure 9 shows that the predicted free energy in this blend at 150 °C is negative for all compositions. The free energy approaches a minimum of −17.5 cal/cm^3 when the PVPh content is around 50 wt %. Therefore, we confirm that the PVPh/PVP is miscible due to the negative free energy and the positive second derivative of weight fraction over the entire compositions.

Conclusions

The PVPh is completely miscible with PVP over entire compositions due to strong hydrogen bonding between the hydroxyl group of PVPh and the carbonyl group of PVP. The Kwei equation can accurately predict T_g's from the experimental results. FTIR and solid-state NMR studies provide positive evidence of the hydrogen bonding between the PVPh hydroxyl group and the PVP carbonyl group. According to the PCAM, the interassociation constant for the PVPh/PVP blend is significantly higher than the self-association constant of PVPh, revealing that the tendency toward hydrogen bonding of the PVPh and PVP dominates the intra-hydrogen bonding of the PVPh in the mixture. In addition, the negative free energy and positive second derivative of weight fraction cover the entire composition. This result indicates that the PVPh/PVP blend is totally miscible, consistent with the DSC analyses.

Acknowledgment. The authors thank the National Science Council, Taiwan, Republic of China, for financially supporting this research under Contract NSC-89-2216-E-009-026.

References and Notes

(1) Chu, P. P.; Wu, H. D. *Polymer* **2000**, *41*, 101.
(2) Miyoshi, T.; Takegoshi, K.; Hikichi, K. *Polymer* **1996**, *37*, 11.
(3) Brus, J.; Dybal, J.; Schmidt, P.; Kratochvil, J.; Baldrain, J. *Macromolecules* **2000**, *33*, 6448.
(4) Coleman, M. M.; Graf, J. F.; Painter, P. C. *Specific Interactions and the Miscibility of Polymer Blends;* Technomic Publishing: Lancaster, PA, 1991.
(5) Zheng, S.; Guo, Q.; Mi, Y. *J. Polym. Sci., Polym. Phys. Ed.* **1999**, *37*, 2412.
(6) Nishio, Y.; Haratani, T.; Takahashi, T. *J. Polym. Sci., Polym. Phys. Ed.* **1990**, *28*, 355.
(7) Ilarduya, A. M.; Iruin, J. J.; Fernandez-Berridi, M. J. *Macromolecules* **1995**, *28*, 3707.
(8) Ceccorulli, G.; Pizzoli, M.; Scandola, M.; Alfonso, G.; Turturro, A. *Polymer* **1989**, *27*, 1195.
(9) Etxeberria, A.; Guezala, S.; Iruin, J. J.; Campa, J. G.; Abajo, J. D. *Polymer* **1998**, *39*, 1035.
(10) Mekhilef, N.; Hadjiandreou, P. *Polymer* **1995**, *36*, 2165.
(11) Qin, C.; Pires, A. T. N.; Belfiore, L. A. *Macromolecules* **1991**, *24*, 666.
(12) Coleman, M. M.; Yang, X.; Painter, P. C.; Graf, J. F. *Macromolecules* **1992**, *25*, 4414.
(13) Wang, J.; Cheung, M. K.; Mi, Y. *Polymer* **2001**, *42*, 2077.
(14) Hill, D. J. T.; Whittaker, A. K.; Wong, K. W. *Macromolecules* **1999**, *32*, 5285.
(15) Zhong, Z.; Guo, Q.; Mi, Y. *Polymer* **1998**, *40*, 27.
(16) Zhang, X.; Takegoshi, K.; Hikichi, K. *Macromolecules* **1991**, *24*, 5756.
(17) Kwei, T. J. *Polym. Sci., Polym. Lett. Ed.* **1984**, *22*, 307.
(18) Moskala, E. J.; Varnell, D. F.; Coleman, M. M. *Polymer* **1985**, *26*, 228.
(19) Hu, Y.; Motzer, H. R.; Etxeberria, A. M.; Fernadez-Berridi, M. J.; Iruin, J. J.; Painter, P. C.; Coleman, M. M. *Macromol. Chem. Phys.* **2000**, *201*, 705.
(20) McBrierty, V. J.; Douglass, D. C. *J. Polym. Sci., Macromol. Rev.* **1981**, *16*, 295.
(21) Demco, D. E.; Johansson, A.; Tegenfeldt, *J. Solid State Nucl. Magn. Reson.* **1995**, *4*, 13.
(22) Clauss, J.; Schmidt-Rohr, K. W. H. *Acta Polym.* **1993**, *44*, 1.

MA010517A